Regular Article

Design, Synthesis and Biological Evaluation of Novel Quinazoline-Based Anti-inflammatory Agents Acting as PDE4B Inhibitors

Rabah Ahmed Taha Serya,*[,a] Abeer Hussin Abbas,[a] Nasser Saad Mohamed Ismail,[a] Ahmed Esmat,[b] and Dalal Abdelrahman Abou El Ella[a]

[a] *Pharmaceutical Chemistry Department, Faculty of Pharmacy, Ain Shams University; ElKhalifa ElMaamoon St., 11566 Abbasseya, Cairo, Egypt: and* [b] *Department of Pharmacology and Toxicology, Faculty of Pharmacy, Ain Shams University; ElKhalifa ElMaamoon St., 11566 Abbasseya, Cairo, Egypt.*

Received October 23, 2014; accepted November 12, 2014

A novel series of quinzoline based compounds (IIIa–d, VIa–f, IXa–f) were designed, synthesized and screened for their inhibitory activity towards the PDE4B isoform. The *in vivo* anti-inflammatory effect of the titled compounds (IIIa–d, VIa–f, IXa–f) as well as their effect on the level of tumor necrosis factor (TNF-α) were evaluated. Among all of the synthesized compounds, IXb, IXd and IXf, exhibited good inhibitory activity against PDE4B enzyme with inhibition percentages of 42, 62 and 68%, respectively. Most of the tested compounds showed potent anti-inflammatory activity compared to indomethacin with a marked decrease in TNF-α level. The ulcerogenic effect of the tested compounds was also examined. The gastric mucosa of the tested animals remained intact after oral administration of the hit compounds. Additionally, docking study was used to explore the possible binding mode of the active compounds on the PDE4B enzyme as well as to illustrate the selectivity of the active hits on the PDE4B isoform.

Key words PDE4B inhibition; tumor necrosis factor-α (TNF-α); quinazoline; anti-inflammatory; docking

Inflammation is a self-protection that preserves the integrity of the organisms against physical, chemical, and infective insults. However, the inflammatory response to several insults could erroneously lead to normal tissue damage while the body is trying to heal itself.[1)] The margination of leukocytes, primarily neutrophils, is one of the early cellular inflammatory events.[2)] Tumor necrosis factor-α (TNF-α), a cytokine, plays an important role in inflammation because of its ability to stimulate cytokine release from neutrophils and biosynthesis of chemokines.[3)] Thus this biomedical pathway has been targeted by the anti-inflammatory therapies used in different chronic inflammatory diseases as chronic obstructive pulmonary disease (COPD) and rheumatoid arthritis.

In addition, cyclic AMP (cAMP) and cyclic GMP (cGMP) are key regulators in various signaling pathways in inflammation inducing numerous intracellular responses by transduction of different inflammatory stimuli among which is TNF-α regulation in human monocytes.[4)] High levels of cAMP have been reported to lead to suppress the function of proinflammatory and immunocompetent cells.[5)] Thus, one of the most important anti-inflammatory targets is to inhibit degradation of c-AMP leading to its accumulation and therefore TNF-α production will be suppressed.[4)] Phosphodiesterases (PDEs) have been known for their ability to degrade cyclic nucleosides.[6)] There are 11 primary families designated (1–11) expressed throughout the human body and having multiple isoforms,[7)] some of which are nonspecific that degrade both c-AMP and c-GMP, others are specific and degrade either one of them.[6,8,9)] The isoform of interest in inflammation is PDE4, as it is involved in regulation of TNF-α production.[4)] PDE4 isoform is comprised of 4 genotype products (PDE4A, PDE4B, PDE4C and PDE4D) and are highly expressed in neutrophils, monocytes, central nervous system (CNS) and smooth muscles of the lung. Literature shows that PDE4B subtype could be a good target for new anti-inflammatory compounds with fewer side effects than already known non-subtype selective PDE4 inhibitors.[7–9)] These side effects, mainly nausea and emesis, considerably limit the use of these drugs. PDE4 inhibitors are very promising compounds, which could bring new alternatives for the treatment of chronic diseases like asthma, COPD, rheumatoid arthritis and atopic dermatitis.[10)] The role of a PDE4B inhibitor is to inhibit c-AMP degradation, thus leading to an increase in c-AMP level thus suppresses TNF-α production in human monocytes.[11)] The first recognized non selective PDE inhibitor was the natural Mesembrine (**1**) which is an alkaloid present in Sceletium tortuosum (kanna)[12)] that has been reported to have a weak PDE4 inhibition.[13)] Rolipram (**2**) was the first synthetically developed first generation PDE4 inhibitor. Unfortunately, its narrow therapeutic index, emesis and other adverse effects limited its use.[14–18)] A breakthrough of PDE4 inhibitors as anti-inflammatory agents came up with second generation Roflumilast (**3**) Dexas® by Merck Sharp & Dohme, a selective, long-acting inhibitor of the enzyme PDE4B.[19–22)] Continuous efforts in this era lead to the discovery of Cilomilast (**4**) Ariflo®, the most advanced PDE4 inhibitor developed by GSK.[10)] Many quinoline based PDE4B inhibitors were also reported in literature among which SCH 351591(**5**) and SCH 365351 (**6**).[23–25)] Further optimization lead to the discovery of the PDE4B inhibitor GSK256066 (**7**) with improved potency optimized for inhaled administration.[26)] Not only quinoline but also some quinazoline based derivatives were reported to have potent PDE4B inhibition such as compounds (**8**–**11**) and (**12**–**14**) that have been recently identified to be selective PDE4B inhibitors in the *in vitro* assay.[27,28)] In addition, nitraquazone having good inhibitory activity with IC_{50}=1.9 μM (**15**) was identified as promising (PDE4) inhibitor.[29)] Moreover 4-substituted-6-nitro quinazoline derivatives compound (**16**) had been reported to inhibit TNF-α production with unique anti-inflammatory effect.[30)] In 2013, 2,4-disubstituted quinazoline derivative E6005 (**17**) was identified to be a

* To whom correspondence should be addressed. e-mail: rabahat2003@yahoo.com

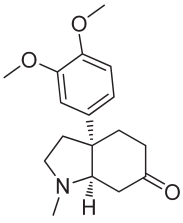

Mesembrine **(1)**

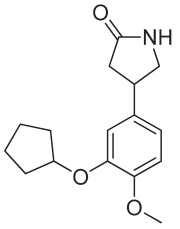

Rolipram **(2)**

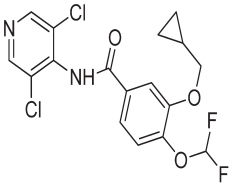

Roflumilast **(3)**

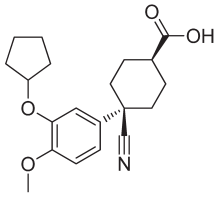

Cilomilast **(4)**

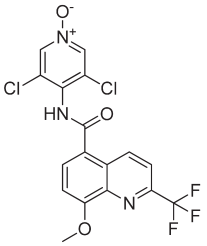

SCH 351591 **(5)**
pIC_{50} (60nM)

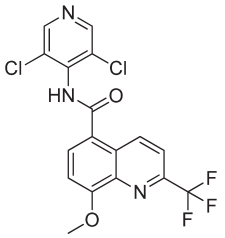

SCH 365351 **(6)**

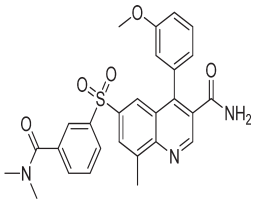

GSK256066 **(7)**
pIC_{50} (11.1nM)

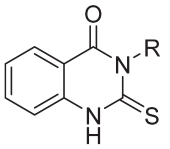

R=Ph	**8**
R=2,6-diFPh	**9**
R=2,3,6-triFPh	**10**
R=2-BrPh	**11**

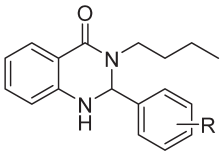

R= 3-OH	**12**
R= 3-F	**13**
R= 3-NO_2	**14**

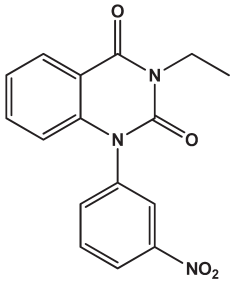

Nitraquazone (15)

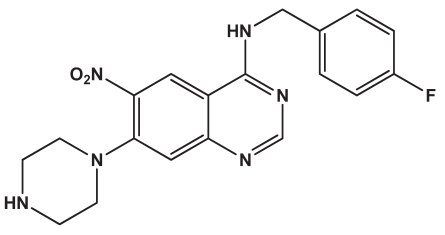

(16)

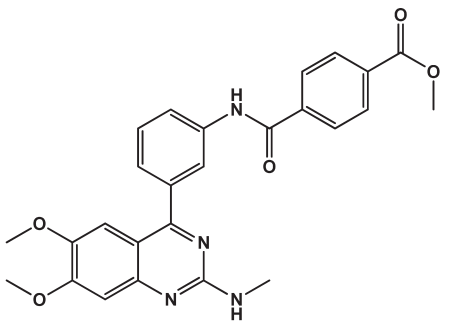

E6005 (17)

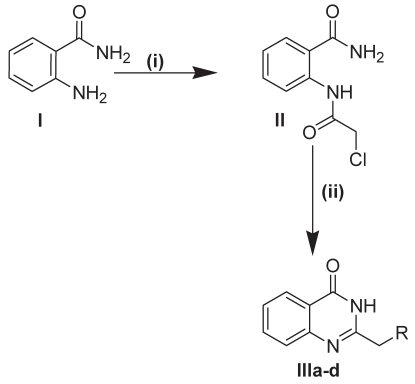

Comp. No.	IIIa	IIIb	IIIc	IIId
R =	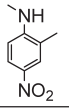	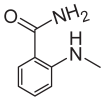	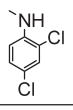	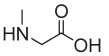

Reagents and conditions: i: Chloroaceyl chloride in benzene, 1 h; ii: R-NH_2, K_2CO_3 in acetonilrile, 6 h reflux.

Chart 1. Synthesis of Compounds **IIIa–d**

potent PDE4 inhibitor with minimal systemic side effects.[31)]

On investigation of the binding site of different isoforms, it was clear that there is a great similarity in the binging site of both PDE4B and PDE4D isoforms, having adenosine recognition site, metal binding pocket and solvent filled side pocket.[32)] Although it was known for decades that the unwanted side effects are mostly attributed to the binding of PDE4 inhibitor to central PDE4D isoform,[33–35)] however, recent studies showed that side effects such as nausea and emesis are more dose dependent rather than binding to the central PDE4D isoform.[36)] The challenge was the development of novel inhibitors against the peripheral PDE4B isoform lacking the ability to cross blood brain barrier aiming to decrease the CNS side effects.

In the present study quinazoline scaffold was used as a main pharmacophoric feature to design selective PDE4B inhibitors. In (Chart 1) series **IIIa–d** was designed using 4-quinazolinone scaffold as potential PDE4B inhibitors which is able to form hydrophobic interactions with the binding pocket.[27)] The design was based on the structural modifications of the reference compound **10** (IC_{50}=13 μM) as a quinazoline based lead compound exhibiting a good PDE4B inhibitory activity.[28)] The modification strategy was based on the replacement of thione moiety with polar amino group as hydrogen bond donor element through one carbon atom spacer and eliminating 3 substituent moiety in reference compound (**10**) aiming to minimize CNS side effects (Fig. 1).

The design of target compounds (**VIa–f** and **IXa–f**, Chart 2 and Chart 3, respectively) was based on the modification of the potent quinazoline based PDE4B inhibitors (**16**)[30)] and (**17**)[31)] as follows (Fig. 2):

a) The quinazoline scaffold was kept as a core which form hydrophobic interactions with the binding pocket and showed hydrogen bonding with Gln443 *via* the N_1 of the heterocyclic ring.[37)]

b) The hydrogen bond formation element was retained at the position number 4 in the quinazoline scaffold through the amine functionality (NH-R) increasing also the polarity of the target compounds as it was reported that aryl polar scaffolds are known to act as selective PDE4B inhibitors.[23)]

c) A nitro group was kept at position 6 of designed target compounds **VIa–f** (Chart 2) as it is reported that the presence of an electron withdrawing group at this position increases the PDE4B inhibitory activity.[38)]

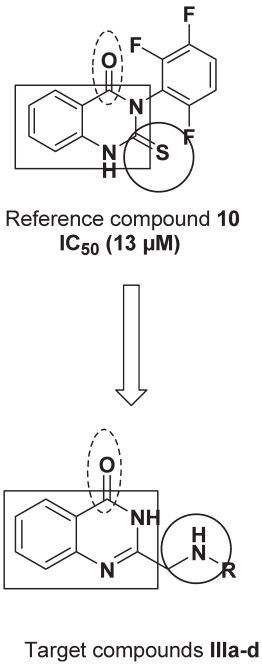

Fig. 1. Design of Proposed Target Compounds **IIIa–d** Based on Molecular Modifications of Reference Compound **10**

Nucleoside binding moiety is shown in rectangular shape, the conserved carbonyl group in oval dashed line shape and the hydrogen bond formation element in circle shape.

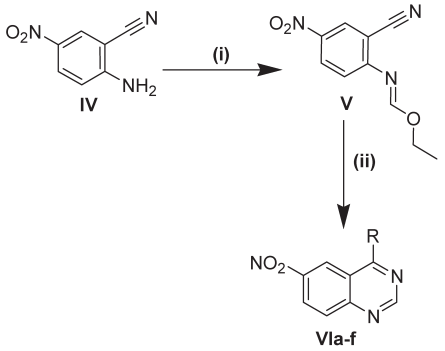

Comp. No.	VIa	VIb	VIc	VId	VIe	VIf
R=					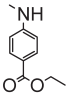	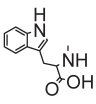

Reagents and conditions: i: Triethyl orthoformate, reflux 16 h, ii: R-NH_2, gl.acetic acid, 1 h.

Chart 2. Synthesis of Target Compounds **VIa–f**

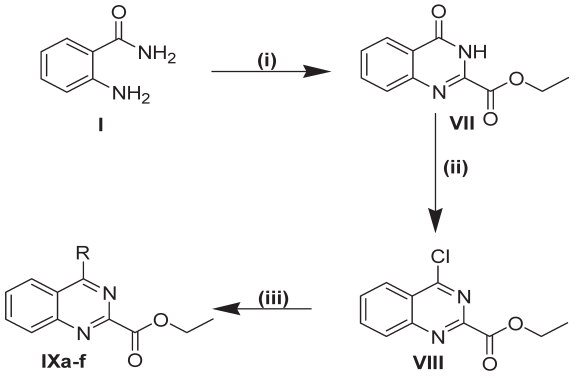

Comp. No.	IXa	IXb	IXc	IXd	IXe	IXf
R=	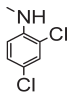	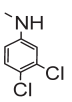	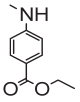	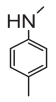		

Reagents and conditions: i: Diethyl oxalate, reflux 6 h, ii: $POCl_3$ in benzene, reflux 6 h, iii: R-NH_2 in ethanol, r.t., 24 h.

Chart 3. Synthesis of Target Compounds **IXa–f**

Results and Discussion

Chemistry Quinazolines have been prepared by different methods in literature allowing variable substitutions at different positions.[39–43] The intermediate compounds (**II**, **V**, **VII** and **VIII**) were prepared as reported and showed similar analytical data.[44–46]

Cyclization of 2-(2-chloroacetamido)benzamide (**II**) with various different amines in acetonitrile in the presence of anhydrous K_2CO_3 and catalytic amount of potassium iodide afforded 2-(aminomethyl) quinazolin-4(3*H*)-one derivatives (**IIIa–d**) (Chart 1). Ring closure of intermediate compound **V** by the reaction with different amines in glacial acetic acid produced 6-nitro 4-substituted amino quinazolines (**VIa–f**) (Chart 2). The reaction of compound **VIII** with different amines in ethanol afforded ethyl 4-(substituted amino) quinazoline-2-carboxylate derivatives (**IXa–f**) (Chart 3). The reaction was activated by the presence of the carboxylate moiety which has (–M) effect that facilitates the release of chlorine as good leaving group. Structural elucidation of the synthesized target compounds **IIIa–d**, **VIa–f** and **IXa–f** was confirmed by different spectral and analytical data.

Biological Evaluation. ***In Vivo*** **Evaluation of the Newly Synthesized Target Compounds** The anti-inflammatory activity of the synthesized compounds (**IIIa–d**, **VIa–f**, **IXa–f**) was first investigated by rat paw edema model followed by measuring the percentage decrease in TNF- α level in the tested lab animals after oral administration of the test compounds (**IIIa–d**, **VIa–f**, **IXa–f**) as stated in ref. 47.

Effect of Test Compounds on Carrageenan-Induced Rat Paw Edema Model: Most of the newly synthesized compounds

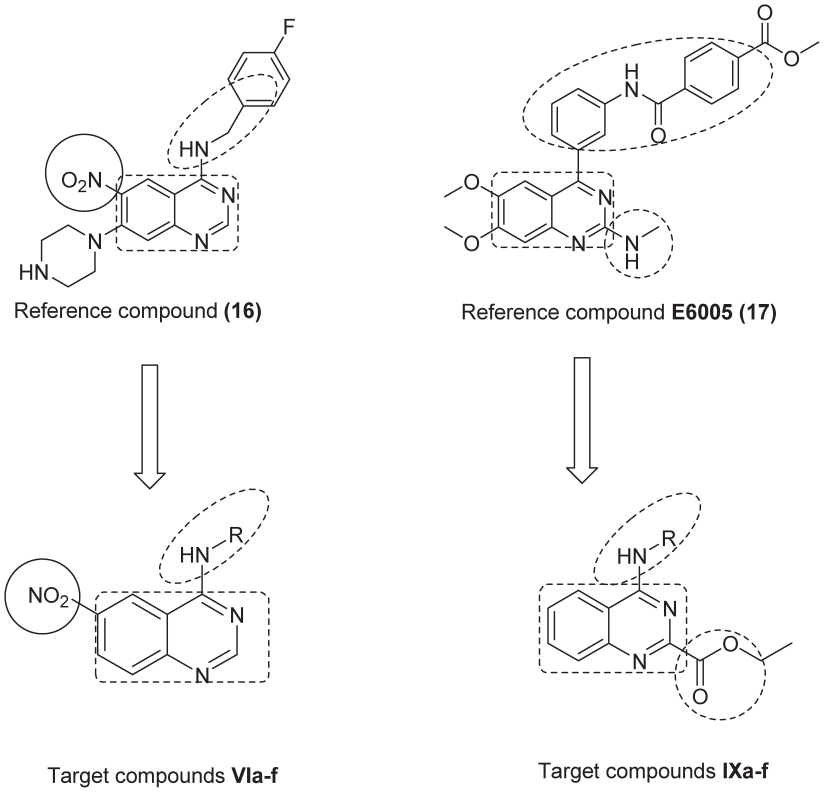

Fig. 2. Design of Proposed Target Compounds **VIa–f** and Target Compounds **IXa–f** Based on Hybridization between Reference Compounds **16** and **17**

Nucleoside binding moiety is shown in rectangle dashed shape, the polar aryl group in oval dashed shape, hydrogen bond formation element in circle dashed shape and the electron withdrawing group in circle solid line shape.

(**IIIa–d**, **VIa–f**, **IXa–f**) were tested for their anti-inflammatory activity against carrageenan induced rat paw edema using indomethacin (10 mg/kg) as potent standard anti-inflammatory drug and using carrageenan for induction of inflammation in the lab animals.[48] The standard dose used of tested compounds was (50 mg/kg).[49] Test compounds were given orally to lab animals followed by injection of the carrageenan, The inhibitory activity of the tested compounds against inflammation was determined by measuring the volume of injected rat paw after 1, 2 and 3 h of carrageenan injection using plethysmometer (Table 1).

The results shown in Table 1 revealed that carragenan caused massive increase in the injected paw volume (about double the volume of the untreated paw in animals of control group). Indomethacin pretreatment (10 mg/kg) produced significant reduction of edema volume in carrageenan treated animals and inhibited edema by 40, 50.7 and 64.38% after 1, 2 and 3 h, as compared to carrageenan group.

The measurement of rat paw volumes and determination of percentage edema inhibition by each of the tested synthesized compounds showed that most of them possess significant anti-inflammatory activity with percentage edema inhibition better than indomethacin after 3 h. Among the tested target compounds **IIIa–d** (Chart 1), compound **IIId** exhibited protection profile 17.14, 56.15 and 71.69% after 1, 2 and 3 h, respectively which reveals that anti-inflammatory action appears after 2 h and increases by time. Regarding the tested target compounds **VIa–f** (Chart 2), compounds **VIb**, **VIc**, **VId** and **VIe** exhibited higher protection compared to indomethacin after 3 h. At the same time compound **VIf** showed comparable protection to that produced by indomethacin after 3 h whereas compound **VIa** showed lower protection than that of indomethacin after 3 h.

The tested compounds **IXa**, **IXb**, **IXd** and **IXf** (Chart 3) showed a good anti-inflammatory activity compared to indomethacin with an inhibitory profile ranging between 68–78% after 3 h of carrageenan injection. Compounds **IXc** and **IXe** showed less anti-inflammatory activity than indomethacin with inhibitory profiles 25.57% and 51.6% after 3 h, respectively.

The Measurement of the Effect of Tested Compounds on TNF-α Level in the Inflammatory Exudates in the Carrageenan Induced Rat Edema Model: Inflammatory exudates from rat paws were used to measure TNF-α released *via* sandwiched enzyme-linked immunosorbent assay (ELISA) technique[50] using TNF-α kits for rats from Raybiotech® (Parkway Lane, Norcross GA, U.S.A.).

Carrageenan significantly increased the TNF-α level, as compared to the control group. Moreover, most of the tested compounds caused significant reduction in the TNF-α concentration (ranging between 75.4–107.7% reduction) compared to that obtained by indomethacin (83.76% reduction).

Among all the tested compounds (**IIIa–d**, **VIa–f**, **IXa–f**), compound **IXa** showed the best inhibitory activity against TNF-α as it lowered the TNF-α concentration about four folds than standard indomethacin. The results shown in (Table 2) revealed that carrageenan caused massive increase in the TNF-α level (about six folds the concentration in the exudates of the untreated paw in animals of control group). Indomethacin pretreatment (10 mg/kg) produced significant reduction

Table 1. The Effect of Tested Compounds on Rat Paw Volume in Carrageenan-Induced Rat Edema Model

Group	1 h		2 h		3 h	
	Paw vol. (mL)	% Edema inhibition	Paw vol. (mL)	% Edema inhibition	Paw vol. (mL)	% Edema inhibition
Control	0.66 [b]±0.073	—	0.487[a,b]±0.051	—	0.453[a,b]±0.043	—
Carrageenin (Car.)	0.718[a]±0.144	—	0.703[a,b]±0.104	—	0.818[a,b]±0.108	—
Car.+Indomethacin	0.695[a,b]±0.046	40%	0.593[a,b]±0.084	50.70%	0.583[a,b]±0.067	64.38%
Car.+**IIIa**	0.715[a,b]±0.036	5.71%	0.672 [a,b]±0.057	14.62%	0.633[a,b]±0.063	50.68%
Car.+**IIIb**	0.712[a,b]±0.056	11.43%	0.675 [a,b]±0.059	13.08%	0.673[a,b]±0.046	39.73%
Car.+**IIIc**	0.715[a,b]±0.069	5.71%	0.665[a,b]±0.172	17.60%	0.707[a,b]±0.161	30.59%
Car.+**IIId**	0.708[a,b]±0.055	17.14%	0.582 [a,b]±0.073	56.15%	0.557[a,b]±0.069	71.69%
Car.+**VIa**	0.703[a,b]±0.071	25.71%	0.613 [a,b]±0.055	41.54%	0.617[a,b]±0.066	55.25%
Car.+**VIb**	0.702[a,b]±0.098	28.57%	0.577 [a,b]±0.107	58.46%	0.552[a,b]±0.091	73.06%
Car.+**VIc**	0.705[a,b]±0.032	22.86%	0.580 [a,b]±0.046	56.92%	0.563[a,b]±0.049	69.86%
Car.+**VId**	0.707[a,b]±0.071	20%	0.603 [a,b]±0.103	46.15%	0.553[a,b]±0.069	72.60%
Car.+**VIe**	0.705 [a,b]±0.061	22.86%	0.623[a,b]±0.1058	36.92%	0.575[a,b]±0.105	66.67%
Car.+**VIf**	0.708[a,b]±0.038	17.14%	0.635 [a,b]±0.050	31.54%	0.595[a,b]±0.035	61.19%
Car.+**IXa**	0.697±0.039	37.14%	0.583±0.078	56.15%	0.533[b]±0.070	78.08%
Car.+**IXb**	0.708±0.107	17.14%	0.618[a,b]±0.092	39.23%	0.57 1[b]±0.084	68.04%
Car.+**IXc**	0.715±0.076	5.71%	0.678[a]±0.045	11.54%	0.725[a]±0.073	25.57%
Car.+**IXd**	0.712±0.101	11.43%	0.648±0.045	25.38%	0.563[b]±0.089	69.86%
Car.+**IXe**	0.703±0.092	25.71%	0.633±0.065	32.31%	0.630[b]±0.121	51.60%
Car.+**IXf**	0.705±0.065	22.86%	0.632±0.072	33.08%	0.543[b]±0.079	75.34%

Data are presented as mean±S.D. Statistical analysis was performed using one-way ANOVA followed by Tukey *post hoc* test. $n=6$. *a*) Statistically different from the corresponding control. *b*) Statistically different from carrageenan-treated group.

Table 2. The Effect of Tested Compounds on TNF-α Level in the Inflammatory Exudates in Carrageenan-Induced Rat Edema Model

Group	TNF-α level	% Decrease in the TNF-α level	Group	TNF-α level	% Decrease in the TNF-α level
Control	2.682[b]±0.343		Car.+**VId**	2.289[b]±0.420	103.58%
Carrageenin (Car.)	13.633[a]±2.631		Car.+**VIe**	2.306[b]±0.450	103.42%
Car.+Indomethacin	4.459[a,b]±0.123	83.76%	Car.+**VIf**	2.695[b]±0.290	99.87%
Car.+**IIIa**	5.374[a,b]±0.563	75.41%	Car.+**IXa**	1.835[b]±0.235	107.72%
Car.+**IIIb**	6.505[a,b]±0.612	65.08%	Car.+**IXb**	2.068[b]±0.296	105.60%
Car.+**IIIc**	6.819[a,b]±1.167	62.21%	Car.+**IXc**	7.783[a,b]±1.038	53.41%
Car.+**IIId**	2.589[b]±0.186	100.83%	Car.+**IXd**	2.344[b]±0.153	103.07%
Car.+**VIa**	4.749[a,b]±1.209	81.12%	Car.+**IXe**	3.062[b]±0.369	96.53%
Car.+**VIb**	2.424[b]±0.396	102.35%	Car.+**IXf**	3.346[b]±0.613	93.93%
Car.+**VIc**	2.369[b]±0.485	102.85%			

Data are presented as mean±S.D. Statistical analysis was performed using one-way ANOVA followed by Tukey *post hoc* test. $n=6$. *a*) Statistically different from the corresponding control. *b*) Statistically different from carrageenan-treated group.

of in TNF-α level in carrageenan treated animals by about three folds as compared to carrageenan group. The measurement TNF-α concentration and percentage decrease of TNF-α level by each of the tested synthesized compounds showed that most of them exhibit significant anti-inflammatory activity with a decrease in TNF-α concentration better than indomethacin. Among the tested target compounds **IIIa–d** (Chart 1), compound **IIId**, which possess an aliphatic substitution at 2-position of quinazoline4-one ring, caused a decrease in TNF-α concentration double that occurred by indomethacin. Nearly all tested target compounds **VIa–f** (Chart 2), compounds **VIb**, **VIc**, **VId**, **VIe** and **VIf** were more effective in lowering TNF-α concentration with the exception to compound **VIa**, with 2-methyl, p-nitro aniline substitution at 4-posistion of quinazoline ring, that caused a comparable decrease in TNF-α concentration to that observed by indomethacin. For tested compounds of Chart 3, only compound **IXc** showed less anti-inflammatory activity than indomethacin.

Acute inflammation such as carrageenan-induced paw edema involves the synthesis or release of mediators at the injured site. Carrageenan-induced paw edema is an experimental animal model for acute inflammation. In the present study, the rat paw edema model showed the ability of prepared target compounds with quinazoline scaffold to significantly reduce paw edema, indicating their potential anti-inflammatory activity. TNF-α is a pleiotropic cytokine that plays a critical role in both acute and chronic inflammation.[51] TNF-α promotes an acute-phase reaction.[52] Several inflammagens have the ability to induce TNF-α synthesis. The formation of several small molecular mediators of inflammation is linked with TNF-α and thus contributes to the range of mediators that critically control inflammation.[53] TNF-α facilitates inflammatory cell infiltration by promoting the adhesion of neutrophils and lymphocytes to endothelial cells.[54] When the TNF-α effect is specifically blocked, the severity of inflammation is reduced.[55] Based on the previous data, it was satisfactory to measure the

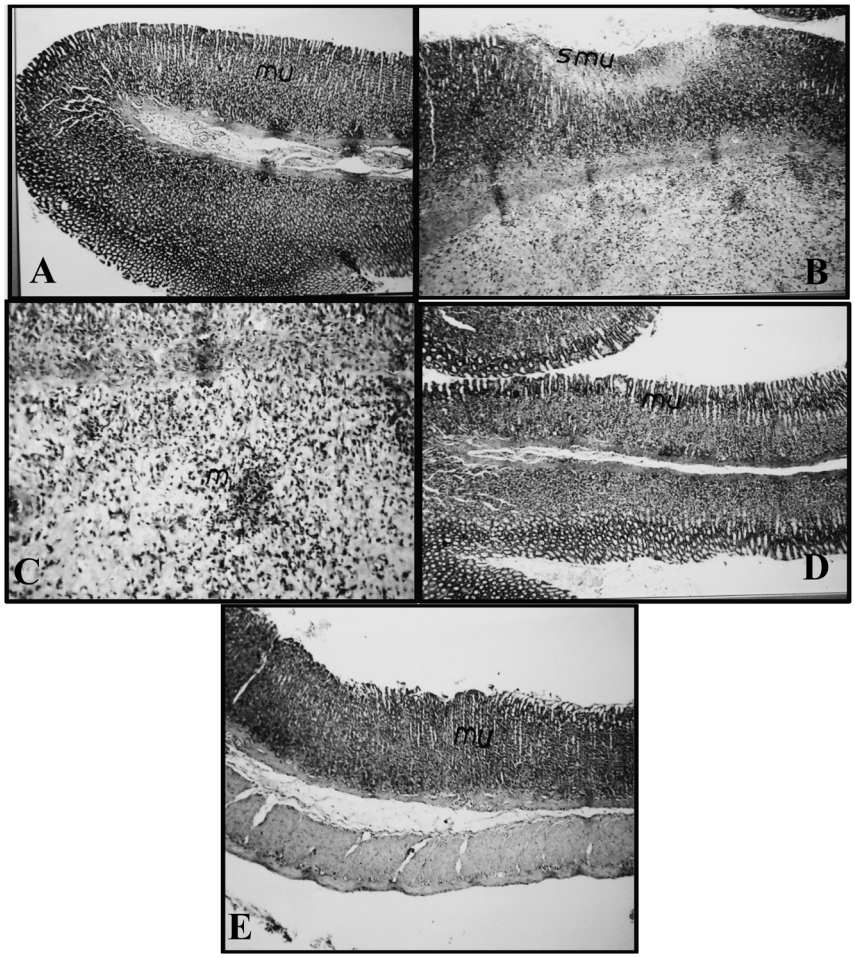

Fig. 3. Histological Section Showing Stomach Mucosa in Different Animal Groups Using Digital Video Camera Mounted at Light Microscope (A–E)

A: Intact stomach mucosa from control group. B: Ulcerated stomach from animals group administrated indomethacin. C: Stomach mucosa from animals group administrated titled compounds **IIId**. D: Stomach mucosa from animals group administrated titled compounds **VIc**. E: Stomach mucosa from animals group administrated titled compounds **IXb**.

Table 3. Ulcer Scores Calculated for Testing Synthesized Compounds Together with Control and Indomethacin as a Reference Compound after Testing on Laboratory Animal Groups

	Control	Indomethacin (Reference drug)	**IIId**	**VIc**	**IXb**
No. of ulcers/rat	0	9	1	2	1
	0	13	2	3	1
	0	9	1	3	1
	0	12	2	2	2
	0	10	2	2	1
	0	12	1	2	2
Ulcer score±S.D.	0	10.833±1.722	1.5±0.547	2.333±0.516	1.333±0.516

levels of TNF-α reduction in the inflammatory exudates in rat paws.

Examination of the Effect of the Prepared Compounds on the Gut Mucosa "Ulcerogenisity Test and Ulcer Index Measurement": Most of the anti-inflammatory medications especially NSAIDS exhibit unwanted side effects such as gastric ulceration and bleeding especially with the prolonged use. From here, there was a concern to discover the effect of the tested target compounds on the gastric mucosa. Histologically examined laboratory animals' stomach showed no ulceration after oral administration of the synthesized target compounds at the effective dose (50 mg/kg) compared to indomethacin administrated group at (10 mg/kg) as shown in (Fig. 3). Inspection of the stained sections revealed obvious ulceration of stomach mucosa or animal group administrated indomethacin compared to the control group. The mucosa of animals in the three groups administrated the prepared target compound showed no ulceration and almost remains intact as that of the control animal group.

The evaluation of the degree of ulceration was expressed in terms of ulcer score, which was calculated by dividing the total number of ulcers in each group by the number of rats in

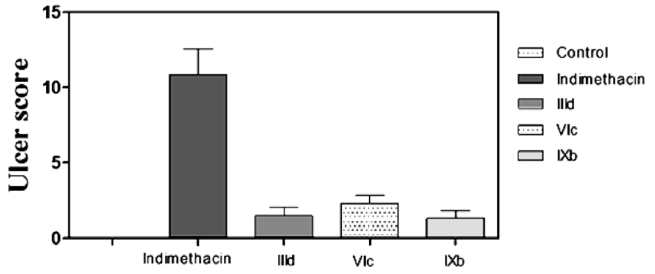

Fig. 4. Ulcer Scores Calculated for Testing Synthesized Compounds together with Control and Indomethacin as a Reference Compound after Testing on Laboratory Animal Groups

Table 4. The Results of Screened Compounds at Concentration of 10 μM over PDE4B Enzyme

Compound ID	% Inhib. 1	% Inhib. 2	Average inhib.
IIId	10	12	11
VIc	8	10	9
VIe	10	8	9
VIf	5	9	7
IXa	21	15	18
IXb	44	40	42
IXd	61	63	62
IXf	69	67	68

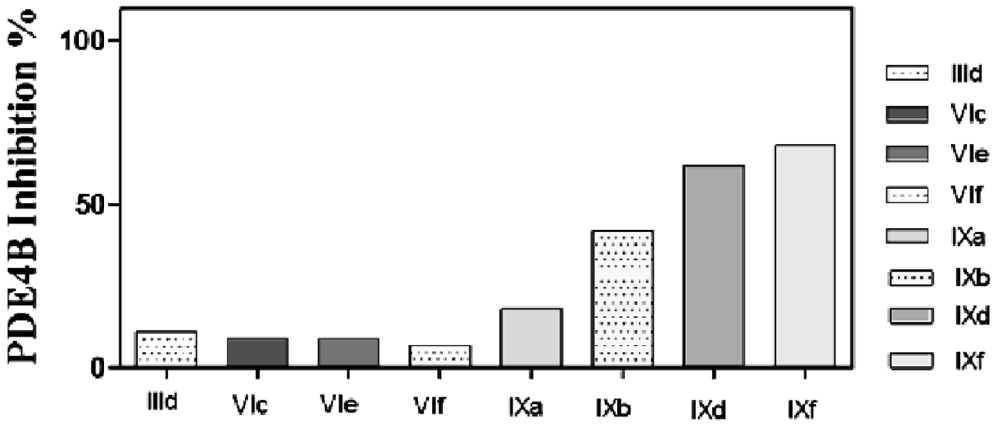

Fig. 5. Results of Screened Compounds at Concentration of 10 μM over PDE4B Enzyme

that group.[56] Titled compound **IIId**, **VIc** and **IXb** were chosen as representative sample of the synthesized target compounds and ulcer scores obtained were as shown in (Table 3, Fig. 4).

***In Vitro* Evaluation of PDE4B Inhibitory Activity** Generally, it has been reported that the PDE4B inhibitory activity of the synthesized compounds could be evaluated at doses up to 100 μM.[57] The inhibitory activity of the newly synthesized compounds (**IIId**, **VIc**,**e**,**f**, **IXa**,**b**,**d**,**f**) which have shown a good TNF-α levels reduction have been evaluated against PDE4B enzyme at doses (10 μM). The assay was conducted by PerkinElmer, Inc. Discovery Services (MD, U.S.A.). A phosphodiesterase-specific compound trequistin was used as a reference in the assay. Compounds (**IXb**, **IXd** and **IXf**) revealed good inhibitory activity at (10 μM) with inhibition percent 42, 62, and 68%, respectively (Table 4, Fig. 5).

Molecular Docking Study Molecular docking study was carried out to all newly synthesized target compounds (**IIIa–d**, **VIa–f**, **IXa–f**) using GOLD algorithm under the interface of accelry's discovery studio 2.5. The docking study of new selective PDE4 inhibitors was facilitated by the published crystal structures of PDE4.[32,58,59] The docking results showed good correlation between the enzymatic activity of our compounds and their binding interactions as well as their Gold Fitness scores.

In the present study, quinoline lead GSK256066 (**7**) that was co-crystallized with the 3D-structure obtained from the protein data bank (Code: 3GWT)[37] was used a reference compound to evaluate the molecular modeling docking study results.

In order to validate the docking algorithm on the target enzyme, the co-crystallized ligand was extracted and re-docked in the active site using GOLD and the docking pose was compared to the original crystal structure. RMSD calculation revealed a value of 0.3Å indicating the ability of the docking algorithm to accurately predict the binding mode of inhibitors in this binding site. Structural analysis of many PDE4B inhibitor complexes has identified two common features.[60] The molecular modelling study showed two main features at the active site, the π–π interactions of planar quinazoline scaffold with the Phe446 by defined as nucleoside binding region and the hydrogen bonding with the invariant glutamine residue (Gln443) that is very essential for activity. It is essential to mention that the loss of that hydrogen bonding in the PDE4B inhibitor diminishes the activity. Representation of the 3D binding mode of GSK256066 (**7**) after docking using GOLD is shown in (Suppl. 1). The molecular modeling study revealed that compounds (**IXb**, **IXd** and **IXf**) which exhibited high inhibition percent against PDE4B enzyme showed comparable Gold Fitness scores relative to the quinoline based GSK256066 (**7**) (Table 5).

Compounds **IXb** and **IXd** (Figs. 6, 7, respectively) showed π–π interaction with Ile410 in addition to the interactions with the essential Phe446. Also, the aryl amine at the 4-position of the quinazoline ring of compound **IXb** showed a third π–π interaction with Met347. Regarding compound **IXf**, and extra hydrogen bonding was clear with Gln443 through the carbonyl moiety at 2-position in addition to the original H-bonding with N_1 of the quinazoline ring (Fig. 8).

Molecular Modelling Study of Selectivity of Hit Compounds for PDE 4B Isoform In 2014,[61] literature reported that ligands with binding modes similar to compound (**18**) (**A33**) would provide another level of specificity by only en-

Table 5. Goldscore Fitness of the Synthesized Compounds and the Percentage PDE4B Inhibition of Screened Compounds

Compound ID	Goldscore fitness	Inhibition of PDE4B	Compound ID	Goldscore fitness	Inhibition of PDE4B
Compound (**7**)	**43.6**	n.t.	**VIe**	38.5	9%
IIIa	37.1	n.t.	**VIf**	39.2	7%
IIIb	32.5	n.t.	**XIa**	44.2	18%
IIIc	31.4	n.t.	**XIb**	44.7	42%
IIId	39.2	11%	**XIc**	35.4	n.t.
VIa	41.5	n.t.	**XId**	45.6	62%
VIb	39.1	n.t.	**XIe**	42.8	n.t.
VIc	37.4	9%	**XIf**	44.1	68%
VId	38.1	n.t.			

All the inhibitory activity shown at 10 μM. n.t.: Not tested.

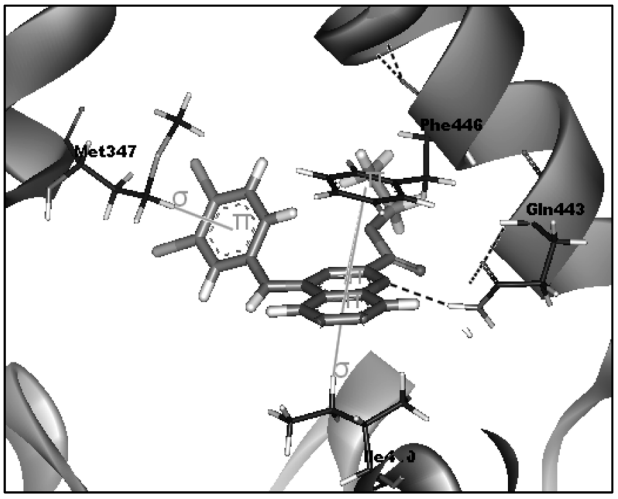

Fig. 6. 3D Diagram of Compound **IXb** at PDE4B Active Site (PDB Code: 3GWT) Showing Interaction of Different Groups with Essential Amino Acids for Inhibitory Activity

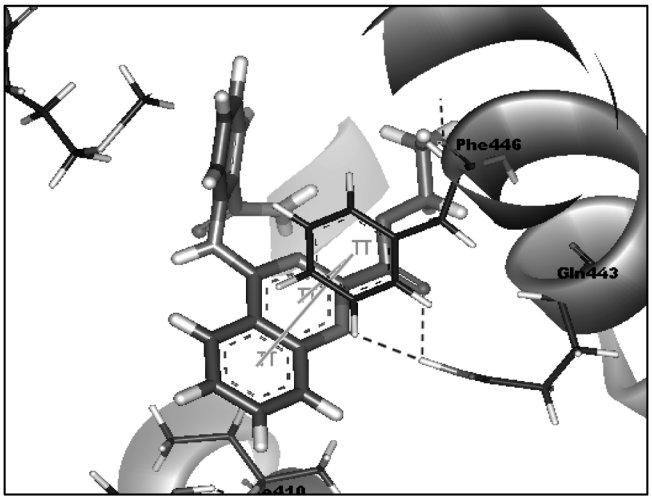

Fig. 8. 3D Diagram of Compound **IXf** at PDE4B Active Site (PDB Code: 3GWT) Showing Interaction of Different Groups with Essential Amino Acids for Inhibitory Activity

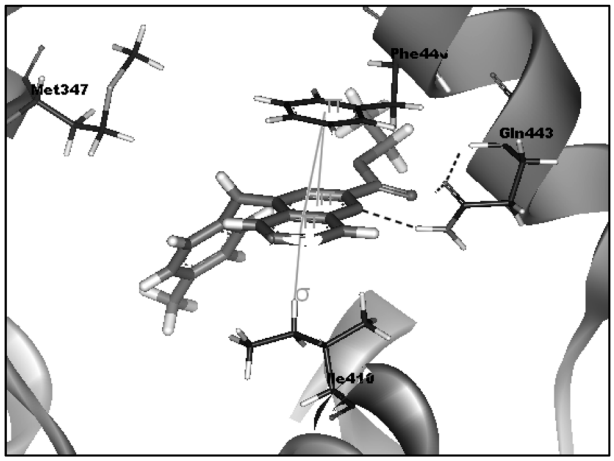

Fig. 7. 3D Diagram of Compound **IXd** at PDE4B Active Site (PDB Code: 3GWT) Showing Interaction of Different Groups with Essential Amino Acids for Inhibitory Activity

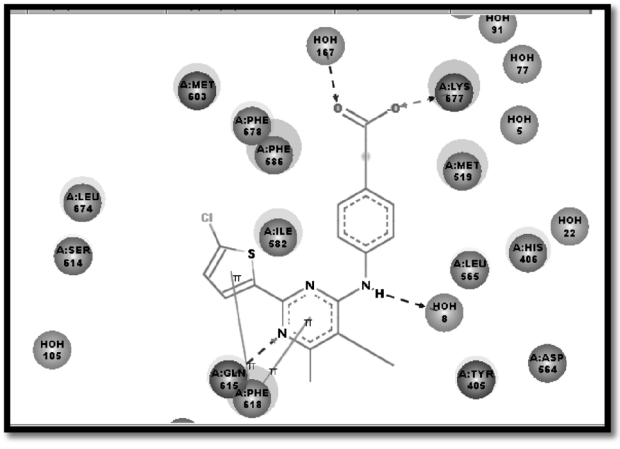

Fig. 9. 2D Interaction Diagram of Compound **18** (**A33**) with PDE4B Active Site (PDB Code: 4MYQ)

gaging a specific subset of PDE4B-partner protein complexes. Therefore molecular docking study was fulfilled to study the binding mode of compound (**18**) (**A33**) and compare it to synthesized and biologically evaluated compounds.

Docking study using PDB coded (4MYQ) showed that compound (**18**) (**A33**) makes multiple interactions with the catalytic domain and simultaneously with residues from CR3 (Fig. 9).

Compound (**18**) (**A33**) binds the PDE4B catalytic domain with its central pyrimidine ring and theinyl ring forming π interactions with Phe618 and in position to hydrogen bond to Gln615. The primary substituent responsible for PDE4B selectivity is arylcarboxymethyl substituents. This group spe-

cifically interacts by making hydrogen bond with amine of Lys677 residue from CR3. The amine of Lys677 directly ties CR3 to the catalytic domain. This interaction is reported be to have a significant effect on the overall binding energy of the closed complex (**18**/catalytic domain/CR3). Together, these results show that compound (**18**) has good shape complementarity as an interface between the catalytic domain and CR3 and makes multiple hydrophobic and polar interactions with both domains. This holds CR3 in a "closed conformation" that blocks substrate binding.[62)]

Investigation of binding mode of our biologically active compounds **IXf** (Fig. 10) and **IXd** (Fig. 11) which exhibited good inhibitory activity against PDE4B enzyme with inhibition percent 62% and 68% to active site revealed that both compounds have the same binding mode as compound **A33** (**18**) (**A33**).

In both compounds the quinazoline ring makes a π interaction with Phe618 which is matched with the thiophene ring of compound **A33** (**18**) making the same π interaction with Phe618, the N1 of quinazoline ring in **IXf** and **IXd** replaced N of pyrimidine ring of (**18**) in making H-bond with Gln615

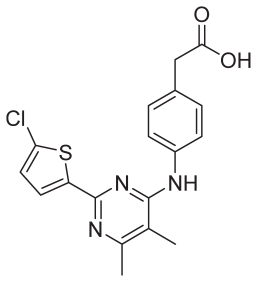

A33 (18)

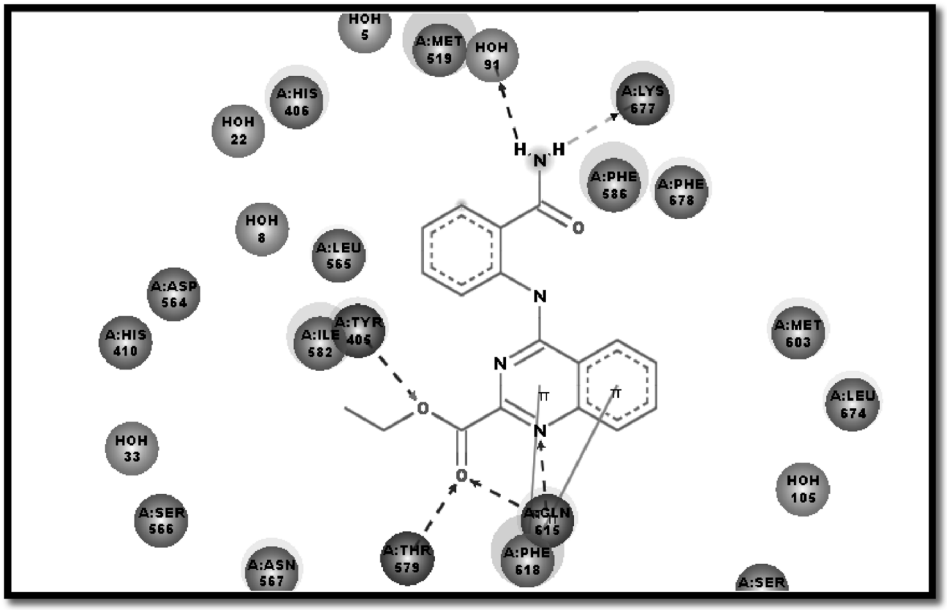

Fig. 10. 2D Interaction Diagram of Compound **IXf** with PDE4B Active Site (PDB Code: 4MYQ)

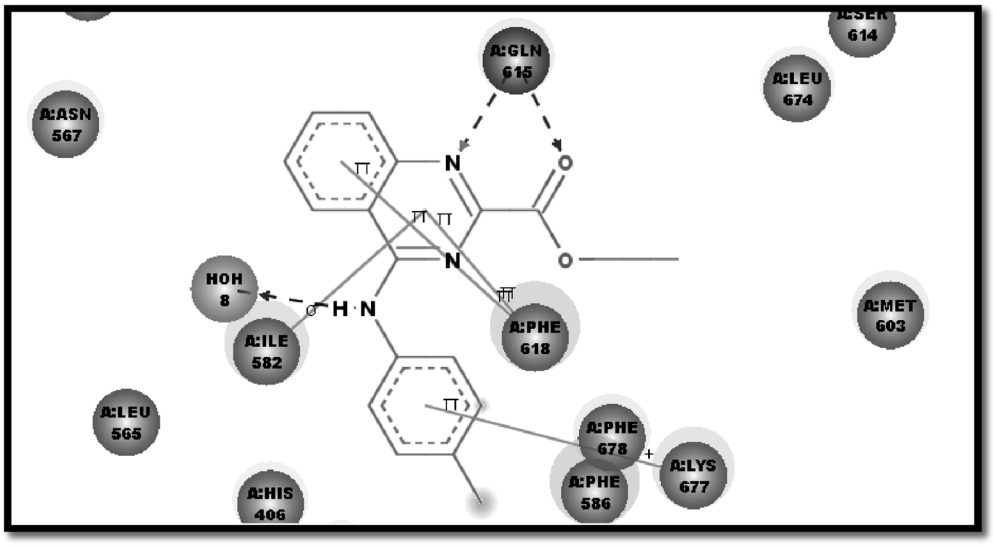

Fig. 11. 2D Interaction Diagram of Compound **IXd** with PDE4B Active Site (PDB Code: 4MYQ)

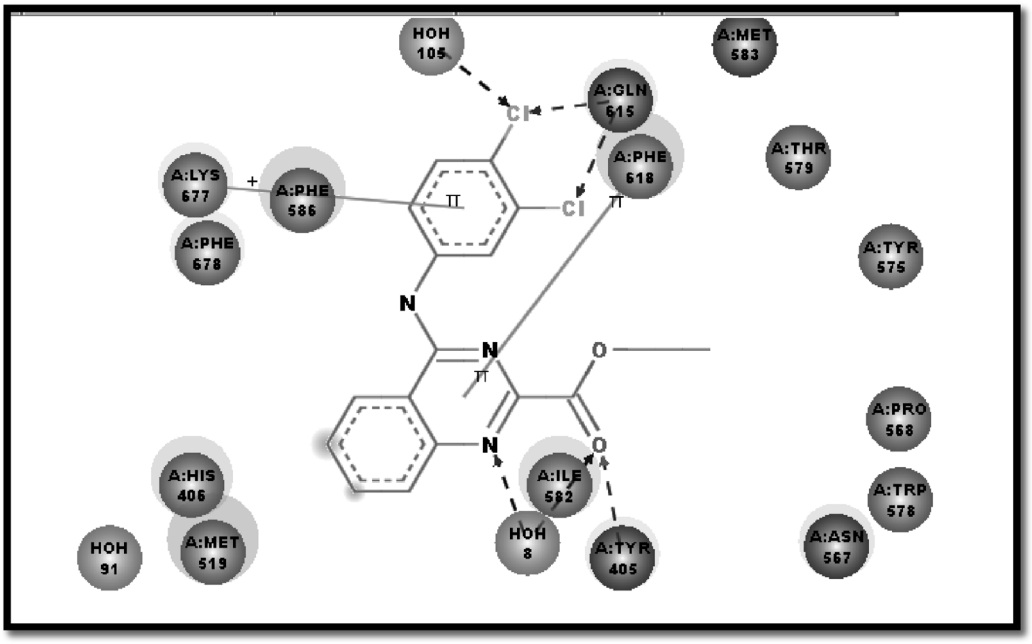

Fig. 12. 2D Interaction Diagram of Compound **IXb** with PDE4B Active Site (PDB Code: 4MYQ)

with extra hydrogen bonding with the same amino acid from carbonyl moiety of ester group. Regarding the CR3, both compounds have the same binding mode with Lys677 by H-bonding with amide NH in **IXf** and aniline phenyl ring of **IXd** respectively. Regarding compound **IXb** which exhibited 42% enzyme inhibition, it showed slightly different binding pattern than **IXf** and **IXd** as shown in (Fig. 12) which may explain lower enzyme inhibition percentage. In **IXb** quinazoline ring made π interaction with Phe618 and aniline phenyl ring made π interaction with Lys677 but the interaction with Gln615 was made by chlorine atoms rather by N_1 of quinazoline ring in **IXf** and **IXd**.

This binding mode of the selected hits was matched with biological results and may indicate that they could have high selectivity for PDE 4B.

Figure 13 shows alignment of compound **IXf** which has the highest enzyme inhibition with compound (**18**) (**A33**) which illustrate that quinazoline ring in **IXf** is perfectly aligned with pyrimidine and thiophene ring in (**A33**). Moreover, aniline ring of both compounds are perfectly aligned together.

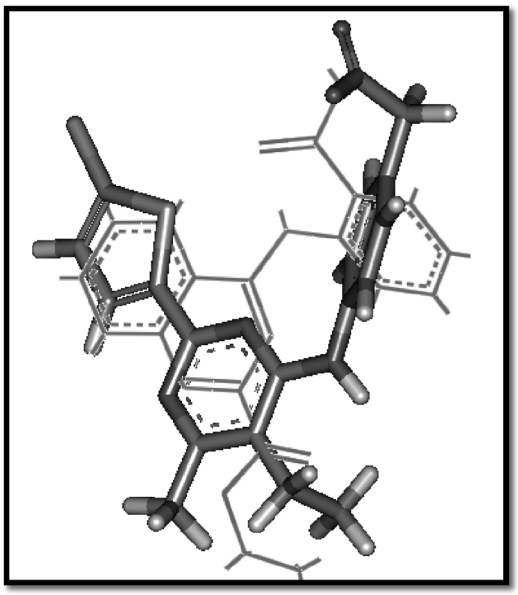

Fig. 13. Alignment of **IXf** (with Line Shaped Bonds) with Compound **18** (with Stick Shaped Bonds)

Conclusion

Out of the prepared compounds, 4-substituted quinazoline 2-carboxylate derivatives (**IXb**, **IXd** and **IXf**) were found to be the most active compounds. This was proved biologically *via in vivo* assays as Rat Paw edema test and measurement of the level of decrease of TNF-α, the important cytokine released during inflammation. *In vitro* assay was carried out by measurement of the enzyme inhibition of our compounds and they have shown remarkable inhibition. Also, the molecular modeling study using GOLD was able to illustrate the good inhibitory of the synthesized compounds as well as high selectivity of these active hits to PDE4B isoform. Additionally, the substitution at the 4-anilino moiety has a great influence on the PDE4B inhibitory activity. The presence of *p*-methyl or *o*-carboxamido on the aniline moiety together with the presence of the ethyl carboxylate moiety at the 2-position of the quinazoline ring seems to play an important role in PDE4B inhibition.

Experimental

Chemistry All the starting materials were purchased from Sigma-Aldrich (U.S.A.). Melting points were determined on Stuart Scientific apparatus and uncorrected. Reactions were monitored using thin layer chromatography (TLC), performed on 0.255 mm silica gel plates (Merck®), with visualization under UV light (254 nm). FT-IR spectra were recorded on a Perkin-Elmer spectrophotometer. ^{1}H-NMR spectra were recorded in δ scale on a Perkin-Elmer 300 MHz spectrometer at Cairo University. EI-MS spectra were recorded on Finnigan Mat SSQ 7000 (70 eV) mass spectrometer, Cairo University.

Elemental analyses were performed at the Microanalytical Center, Cairo University.

The intermediate compounds (**II**, **V**, **VII** and **VIII**) were prepared as reported and showed similar analytical data.[44–46]

Preparation of 2-((4-Oxo-3,4-dihydroquinazolin-2-yl) methyl) Amino Derivatives (IIIa–c) (General Procedure) A mixture of **II** (0.85 g, 4.00 mmol) and the respective amine (4.00 mmol) in the presence of K_2CO_3 (6.00 mmol) and KI (0.20 mmol) was refluxed in acetonitrile (10 mL) for 6 h. After that, the solvent was evaporated under reduced pressure, and then the residue was triturated with cooled dil HCl (10%). The precipitate was then filtered and washed with diethyl ether and crystallized from ethylacetate to yield titled compounds **IIIa–d**.

2-(((2-Methyl-4-nitrophenyl)amino)methyl)quinazolin-4(3*H*)-one (**IIIa**): Yellow crystals (60%); mp: 118–120°C; FT-IR (ν^- max, cm^{-1}): 3466 (N-H), 1505 and 1382 (NO_2); ^{1}H-NMR (300 MHz, DMSO-d_6) δ: 7.88–7.73 (m, 3H, Ar), 7.46–6.65 (m, 4H, Ar), 6.51 (s, 1H, NH), 5.35 (s, 1H, NH), 3.50 (s, 2H, $\underline{CH_2}$-NH), 2.08 (s, 3H, $\underline{CH_3}$-Ar); MS: *m/z* (%) 310 [M^+, (38.00%)]; *Anal*. Calcd for $C_{16}H_{14}N_4O_3$: C, 61.93; H, 4.55; N, 18.06. Found: C, 61.74; H, 4.56; N, 18.11.

2-(((4-Oxo-3,4-dihydroquinazolin-2-yl)methyl)amino)benzamide (**IIIb**): White crystals (50%); mp: 125–128°C; FT-IR (ν^- max, cm^{-1}): 3347–3107 (N-H, N-H_2 forked), 1710 (C=O amide), 1648 (C=O amide); ^{1}H-NMR (300 MHz, DMSO-d_6) δ: 8.90 (s, 2H, NH_2), 8.10–6.81 (m, 8H, Ar), 6.74 (s, 1H, NH), 6.55 (s, 1H, NH), 4.31 (s, 2H, NH-$\underline{CH_2}$); MS: *m/z* (%) 294 [M^+, (23.42%)]; *Anal*. Calcd for $C_{16}H_{14}N_4O_2$: C, 65.30; H, 4.79; N, 19.04. Found: C, 65.57; H, 4.61; N, 19.23.

2-(((2,4-Dichlorophenyl)amino)methyl)quinazolin-4(3*H*)-one (**IIIc**): Yellow crystals (60%); mp: 220–223°C; FT-IR (ν^- max, cm^{-1}): 3340 (N-H), 1714 (C=O amide); ^{1}H-NMR (300 MHz, DMSO-d_6) δ: 8.38–6.95 (m, 7H, Ar), 6.36 (s, 1H, NH), 5.59 (s, 1H, NH), 4.19 (s, 2H, NH-$\underline{CH_2}$); MS: *m/z* (%) 320 [M^+, (13.00%); *Anal*. Calcd for $C_{15}H_{11}Cl_2N_3O$: C, 56.27; H, 3.46; N, 13.12. Found: C, 56.51; H, 3.53; N, 13.06.

2-(((4-Oxo-3,4-dihydroquinazolin-2-yl)methyl)amino)acetic acid (**IIId**): White crystals (50%); mp: 158–160°C; FT-IR (ν^- max, cm^{-1}): 3369–3410 (OH carboxylic), 3283–3197 (N-H), 1682 (C=O acid), 1648 (C=O amide); ^{1}H-NMR (300 MHz, DMSO-d_6) δ: 12.22 (s, 1H, OH), 11.90 (s, 1H, NH), 8.39–7.09 (m, 4H, Ar), 4.91 (s, 1H, NH), 2.88 (s, 2H, $\underline{CH_2}$-NH), 3.50 (s, 2H, $\underline{CH_2}$-COOH); MS: *m/z* (%) 233 [M^+, (10.00%)]; *Anal*. Calcd for $C_{11}H_{11}N_3O_3$: C, 56.65; H, 4.75; N, 18.02. Found: C, 56.56; H, 4.78; N, 18.17.

Preparation of 6-Nitro 4-Substituted Amino Quinazoline Derivatives (VIa–f) (General Procedure) A mixture of **V** (1.01 g, 5.00 mmol) with the respective amine (5.00 mmol) in glacial acetic acid (10 mL) was refluxed for 1 h. The reaction mixture was then allowed to cool and the precipitate was collected by filtration, washed with diethyl ether and crystallized from ethanol to afford titled compounds **VIa–f**.

N-(2-Methyl-4-nitrophenyl)-6-nitroquinazolin-4-amine (**VIa**): Yellow crystals (70%); mp: 190–192°C; FT-IR (ν^- max, cm^{-1}): 3330 (N-H), 1573 and 1314 (NO_2); ^{1}H-NMR (300 MHz, DMSO-d_6) δ: 9.16 (s, 1H, NH), 8.74–8.36 (m, 2H, quinazoline Ar H), 8.45 (s, 1H, quinazoline Ar-H), 2.58 (s, 3H, Ar-$\underline{CH_3}$); 7.8–7.1 (m, 3H, Ar-H), 8.29 (s, 1H, quinazoline-H), MS: *m/z* (%) 325 [M^+, (4.58%)]; *Anal*. Calcd for $C_{15}H_{11}N_5O_4$: C, 55.39; H, 3.41; N, 21.53. Found: C, 55.21; H, 3.36; N, 21.36.

2-((6-Nitroquinazolin-4-yl)amino)benzamide (**VIb**): Yellow crystals (70%); mp: 268–270°C; FT-IR (ν^- max, cm^{-1}): 3416–3399 (NH, NH_2), 1681 (C=O amide); ^{1}H-NMR (300 MHz, DMSO-d_6) δ: 11.21 (s, 2H, NH_2), 10.71 (s, 1H, NH), 8.44–8.26 (m, 2H, quinazoline Ar H), 8.73 (s, 1H, quinazoline Ar-H), 8.49 (s, 1H, quinazoline-H), 7.23–6.90 (m, 4H, Ar); MS: *m/z* (%) 309 [M^+, (64.80%)]; *Anal*. Calcd for $C_{15}H_{11}N_5O_3$: C, 58.25; H, 3.58; N, 22.64. Found: C, 58.39; H, 3.54; N, 22.58.

N-(2,4-Dichlorophenyl)-6-nitroquinazolin-4-amine (**VIc**): Yellow crystals (70%); mp: 198–200°C; FT-IR (ν^- max, cm^{-1}): 3408 (N-H), 1575 and 1323 (NO_2); ^{1}H-NMR (300 MHz, DMSO-d_6) δ: 10.61 (s, 1H, NH), 8.74–8.42 (m, 2H, quinazoline Ar H), 8.43 (s, 1H, quinazoline Ar-H), 8.38 (s, 1H, quinazoline-H), 7.23–6.90 (m, 3H, Ar); MS: *m/z* (%) 335 [M^+, (7.58%)], *Anal*. Calcd for $C_{14}H_8Cl_2N_4O_2$: C, 50.17; H, 2.41; N, 16.72. Found: C, 50.36; H, 2.21; N, 16.45.

N-(3,4-Dichlorophenyl)-6-nitroquinazolin-4-amine (**VId**): Yellow crystals (70%); mp: 200–203°C; FT-IR (ν^- max, cm^{-1}): 3408 (N-H), 1497 and 1323 (NO_2); ^{1}H-NMR (300 MHz, DMSO-d_6) δ: 10.69 (s, 1H, NH), 8.74–8.32 (m, 2H, quinazoline Ar H), 8.33 (s, 1H, quinazoline Ar-H), 8.48 (s, 1H, quinazoline-H), 7.23–6.77 (m, 3H, Ar); MS: *m/z* (%) 335.00 [M^+, (16.04%)]; *Anal*. Calcd for $C_{14}H_8Cl_2N_4O_2$: C, 50.17; H, 2.41; N, 16.72. Found: C, 50.18; H, 2.31; N, 16.60.

Ethyl 4-((6-nitroquinazolin-4-yl)amino)benzoate (**VIe**): Yellow crystals (70%); mp: 204–206°C; FT-IR (ν^- max, cm^{-1}): 3408 (N-H), 1771 (C=O ester), 1642 (C=N), 1572 and 1319 (NO_2); ^{1}H-NMR (300 MHz, DMSO-d_6) δ: 11.70 (s, 1H, NH), 8.76–8.40 (m, 2H, quinazoline Ar H), 8.73 (s, 1H, quinazoline Ar-H), 8.36 (s, 1H, quinazoline-H), 4.36 (q, J=7.11 Hz, 2H, $\underline{CH_2}$-CH_3), 1.38 (t, J=7.18 Hz, 3H, $\underline{CH_3}$-CH_2); 7.51 (dd, J=7.5, 2H, Ar-H), 7.59 (dd, J=7.5, 2H, Ar-H), MS: *m/z* (%) 338 [M^+, (46.85%)]; *Anal*. Calcd for $C_{17}H_{14}N_4O_4$: C, 60.35; H, 4.17; N, 16.56. Found: C, 60.57; H, 4.24; N, 16.61.

3-(1*H*-Indol-3-yl)-2-((6-nitroquinazolin-4-yl)amino)propanoic acid (**VIf**): Yellow crystals (50%); mp: 185–186°C; FT-IR (ν^- max, cm^{-1}): 3409–3892 broad (OH carboxylic), 3330 (N-H), 1747 (C=O acid), 1498 and 1316 (NO_2); ^{1}H-NMR (300 MHz, DMSO-d_6) δ: 13.10 (s, 1H, OH), 11.07 (s, 1H, NH), 10.90 (s, 1H, NH), 8.56–8.41 (m, 2H, quinazoline Ar H), 8.75 (s, 1H, quinazoline Ar-H), 8.46 (s, 1H, quinazoline-H), 7.64–7.15 (m, 4H, Ar-indole), 7.02 (s, 1H, C=$\underline{CH}$-NH indole), 3.78 (m, 1H, NH-$\underline{CH}$-COOH), 3.20 (d, J=7.90 Hz, 2H, NH-CH-$\underline{CH_2}$); MS: *m/z* (%) 377 [M^+, (21.40%)]; *Anal*. Calcd for $C_{19}H_{15}N_5O_4$: C, 60.47; H, 4.01; N, 16.56. Found: C, 60.28; H, 4.08; N, 16.33.

Preparation of Ethyl 4-(Substituted-amino)quinazoline-2-carboxylate Derivatives (IXa–f) (General Procedure) To a stirred ice cooled solution of the respective amine (1.50 mmol) in ethanol, a cooled solution of **VIII** (0.24 g, 1.00 mmol) in ethanol was added dropwise, the reaction mixture was then allowed to stir for 24 h, after that the solvent was evaporated under reduced pressure, the precipitate was filtered and washed with 10% HCl, diethyl ether and recrystallized from ethanol to yield titled compounds **IXa–f**.

Ethyl 4-((2,4-Dichlorophenyl)amino)quinazoline-2-carboxylate (**IXa**): Yellow crystals (50%); mp: 185–186°C; FT-IR (ν^- max, cm^{-1}) : 3423 (N-H), 1685 (C=O ester); ^{1}H-NMR (300 MHz, DMSO-d_6) δ: 11.13 (s, 1H, NH), 7.90–6.59 (m, 7H, Ar), 4.3 (q, J=7.11 Hz, 2H, $\underline{CH_2}$-CH_3), 1.57 (t, J=7.13 Hz, 3H,

CH_2-$\underline{CH_3}$); MS: *m/z* (%) 362 [M^+, (62.5%)], *Anal*. Calcd for $C_{17}H_{13}Cl_2N_3O_2$: C, 56.37; H, 3.62; N, 11.60. Found: C, 56.11; H, 3.51; N, 11.65.

Ethyl 4-((3,4-Dichlorophenyl)amino)quinazoline-2-carboxylate (**IXb**): Yellow crystals (50%); mp: 212–213°C; FT-IR (ν^- max, cm^{-1}): 3381 (N-H), 1699 (C=O ester); δ 11.07 (s, 1H, NH), 7.30–6.71 (m, 7H, Ar), 4.37 (q, *J*=7.11 Hz, 2H, $\underline{CH_2}$-CH_3), 1.31 (t, *J*=7.10 Hz, 3H, CH_2-$\underline{CH_3}$); MS: *m/z* (%) 362 [M^+, (14.29%)]; *Anal*. Calcd for $C_{17}H_{13}Cl_2N_3O_2$: C, 56.37; H, 3.62; N, 11.60. Found: C, 56.28; H, 3.64; N, 11.52.

Ethyl 4-((4-(Ethoxycarbonyl)phenyl)amino)quinazoline-2-carboxylate (**IXc**): White crystals (60%); mp: 187–190°C; FT-IR (ν^- max, cm^{-1}): 3418 (N-H), 1718 (C=O ester, ketone); ^{1}H-NMR (300 MHz, DMSO-d_6) δ: 11.35 (s, 1H, NH), 8.03–7.40 (m, 4H, quinazoline-Ar), 7.61 (dd, *J*=7.5, 2H, Ar-H), 7.57 (dd, *J*=7.5, 2H, Ar-H), 4.43 (q, *J*=7.10 Hz, 4H, $\{\underline{CH_2}$-$CH_3\}_2$), 1.36 (t, *J*=7.11 Hz, 6H, $\{CH_2$-$\underline{CH_3}\}_2$); MS: *m/z* (%) 365 [M^+, (93.33%)]; *Anal*. Calcd for $C_{20}H_{19}N_3O_4$: C, 65.74; H, 5.24; N, 11.50. Found: C, 65.80; H, 5.26; N, 11.66.

Ethyl 4-(*p*-Tolylamino)quinazoline-2-carboxylate (**IXd**): Yellow crystals (60%); mp: 178–180°C; FT-IR (ν^- max, cm^{-1}): 3360 (N-H), 1726 (C=O ester); ^{1}H-NMR (300 MHz, DMSO-d_6) δ: 10.90 (s, 1H, NH), 8.16–7.28 (m, 4H, quinazoline-Ar), 7.21 (dd, *J*=7.5, 2H, Ar-H), 7.34 (dd, *J*=7.5, 2H, Ar-H), 4.41 (q, *J*=7.13 Hz, 2H, $\underline{CH_2}$-CH_3), 2.37 (s, 3H, $\underline{CH_3}$-Ar), 1.41 (t, *J*=7.12 Hz, 3H, CH_2-$\underline{CH_3}$); MS: *m/z* (%) 307 [M^+, (58.80%)]; *Anal*. Calcd for $C_{18}H_{17}N_3O_2$: C, 70.34; H, 5.58; N, 13.67. Found: C, 69.91; H, 5.16; N, 13.53.

Ethyl 4-(1*H*-Benzo[*d*]imidazol-1-yl)quinazoline-2-carboxylate (**IXe**): White crystals (60%); mp: 170–172°C; FT-IR (ν^- max, cm^{-1}): 1714 (C=O ester), 1630 (C=N); ^{1}H-NMR (300 MHz, DMSO-d_6) δ: 8.61–8.17 (m, 4H, quinazoline-Ar), 8.05–7.64 (m, 4H, Ar-benzimidazole), 8.11 (s, 1H, benzimidazole-H), 4.31 (q, *J*=7.10 Hz, 2H, $\underline{CH_2}$-CH_3), 1.32 (t, *J*=7.10 Hz, 3H, CH_2-$\underline{CH_3}$); MS: *m/z* (%) 318 [M^+, (13.60%)]; *Anal*. Calcd for $C_{18}H_{14}N_4O_2$: C, 67.91; H, 4.43; N, 17.60. Found: C, 67.78; H, 4.58; N, 17.58.

Ethyl 4-((2-Carbamoylphenyl)amino)quinazoline-2-carboxylate (**IXf**) White crystals (60%); mp: 178–180°C; FT-IR (ν^- max, cm^{-1}): 3441–3403 (N-H, N-H_2 forked), 1732 (C=O ester), 1658 (C=O amide); ^{1}H-NMR (300 MHz, DMSO-d_6) δ: 13.30 (s, 2H, NH_2), 10.50 (s, 1H, NH), 8.05–7.15 (m, 8H, Ar), 4.33 (q, *J*=7.10 Hz, 2H, $\underline{CH_2}$-CH_3), 1.35 (t, *J*=7.10 Hz, 3H, CH_2-$\underline{CH_3}$); MS: *m/z* (%) 336 [M^+, (55.56%)], *Anal*. Calcd for $C_{18}H_{16}N_4O_3$: C, 64.28; H, 4.79; N, 16.66. Found: C, 64.25; H, 4.99; N, 16.54.

Biological Evaluation. ***In Vivo*** **Evaluation of Anti-inflammatory Activity** Chemicals: Inflammatory-grade carrageenan was purchased from FMC (Rockland, ME, U.S.A.). All other chemicals were of the highest available commercial grade. All test compounds were dissolved in dimethyl sulfoxide (DMSO) (Sigma-Aldrich, U.S.A.) before being injected into the animals.

Animals: Throughout the experiments, adult male Sprague–Dawley rats weighing 120–150 g were used. They were housed at a temperature of 23±2°C with free access to water and standard food pellets. Rats were acclimatized in our animal facility for at least 1 week prior to the experiment.

Measurement of Paw Volume in Carrageenan-Induced Rat Edema Model: Rats were equally divided into several groups (6 animals /group). The first group was to be used as control group and the second one to be injected with carrageenan only. Animals in the third group were given orally indomethacin as standard anti-inflammatory drug (10 mg/kg). The remaining groups were given orally the test compounds at (50 mg/kg). Dosing volume was kept constant (10 mL/kg). Thirty minutes after oral administration, rats in the first group were injected subcutaneously with 0.05 mL saline, while animals in all other groups injected subcutaneously (s.c.) with 0.05 mL carrageenan (1% solution in saline) on the plantar surface of the right hind paw. The right hind paw volume was measured at 1, 2 and 3 h after carrageenan injection by saline displacement using UGO-BASILE 7140 plethysmometer (Comerio, Italy). The measured volumes were used to calculate % edema inhibition for each compound at each dose level.[63]

Statistical Analysis: Data are presented as mean±S.D. values. Statistical analysis was performed using one-way analysis of variance followed by Tukey–Kramer multiple comparisons tests. The 0.05 level of probability was used as the criterion for significance. All statistical analyses were performed using GraphPad (La Jolla, CA, U.S.A.) InStat software version 3. Graphs were sketched using GraphPad Prism software version 4 (ISI_Software, La Jolla, CA, U.S.A.).

Determination of Rat TNF-α Concentration: The assay was carried out according to the manufacturer recommendations using ELISA kit provided by RayBiotech systems. Briefly, Rat TNF-α level was determined by quantitative sandwich enzyme immunoassay technique. The enzyme reaction yielded a blue product that turned yellow when the stop solution was added. The intensity of the color measured was proportional to the amount of TNF-α bound in the initial step.

Induction of Gastric Ulcer: The animals were fasted for 36 h in separate cages with raised wide wire mesh to avoid coprophagia,[64] but with water given *ad libitum*. After 8 h, animals were sacrified, stomach removed and opened on greater curvature and examined for ulceration. Evaluation of degree of ulceration was expressed in terms of ulcer score which is calculated by dividing the total number of ulcers in each group by number of rats in that group.[65] To get the histological data, representative stomach samples were taken from different group and fixed in 10% formalin in saline for 24 h. Washing was done in tap water then serial dilutions of alcohol (methyl, ethyl and absolute ethyl) were used for dehydration. Specimens were cleared in xylene and embedded in paraffin at 56°C in hot air oven for twenty four hours. Paraffin bees wax tissue blocks were prepared for sectioning at 4 μm thickness by slidge microtome. The obtained tissue sections were collected on glass slides, deparaffinized, stained by hematoxylin and eosin stain then examination was done through using digital video camera mounted at light microscope (CX2, OLYMPUS, Japan).[66]

Measurement of PDE4B Enzyme Inhibitory Activity of Prepared Compounds ***in Vitro*** Methodolgy: The assay was done using the Caliper LabChip 3000 and a 12-sipper LabChip. The separations are based on that the product and substrate are electrophoretically separated. The off-chip incubation mobility-shift phosphodiesterase assay uses a microfluidic chip to measure the conversion of a fluorescent cyclic AMP or GMP substrate to a 5′-AMP or 5′-GMP product. The reaction mixture, from a microtiter plate well, is introduced through a capillary sipper onto the chip, where the fluorescent substrate and product are separated by electrophoresis and de-

tected *via* laser-induced fluorescence.

Materials and Conditions of the Assay: Materials used and the assay conditions for screening of the target compounds over PDE4B as got from PerkinElmer, Inc., Company were to use PDE4B in 0.037 nM and 100 mM *N*-(2-hydroxyethyl)-piperazine-*N*′-2-ethanesulfonic acid (Hepes) (pH=7.5) as buffer, 0.010% Brij as detergent and peptide used was 2.0 μM iFluor 488-AHC-cAMP and trequinsin as reference compound.

Conflict of Interest The authors declare no conflict of interest.

Supplementary Materials The online version of this article contains supplementary materials.

References

1) Maddison P. J., Isenberg D. A., Woo P., Glass D. N., Breedveld F., "Oxford Textbook of Rheumatology," 3rd ed., Oxford University Press, Oxford, U.K., 2004.
2) Goulet J. L., Snouwaert J. N., Latour A. M., Coffman T. M., Koller B. H., *Proc. Natl. Acad. Sci. U.S.A.*, **91**, 12852–12856 (1994).
3) Marucha P. T., Zeff R. A., Kreutzer D. L., *J. Immunol.*, **147**, 2603–2608 (1991).
4) Ochiai H., Odagaki Y., Ohtani T., Ishida A., Kusumi K., Kishikawa K., Yamamoto S., Takeda H., Obata T., Kobayashi K., Nakai H., Toda M., *Bioorg. Med. Chem.*, **12**, 5063–5078 (2004).
5) Dal Piaz V., Giovannoni M. P., *Eur. J. Med. Chem.*, **35**, 463–480 (2000).
6) Soderling S. H., Bayuga S. J., Beavo J. A., *Proc. Natl. Acad. Sci. U.S.A.*, **95**, 8991–8996 (1998).
7) Boswell-Smith V., Spina D., Page C. P., *Br. J. Pharmacol.*, **147** (Suppl. 1), S252–S257 (2006).
8) Conti M., Richter W., Mehats C., Livera G., Park J. Y., Jin C., *J. Biol. Chem.*, **278**, 5493–5496 (2003).
9) Houslay M. D., Adams D. R., *Biochem. J.*, **370**, 1–18 (2003).
10) Hamblin J. N., Angell T. D. R., Ballantine S. P., Cook C. M., Cooper A. W. J., Dawson J., Delves C. J., Jones P. S., Lindvall M., Lucas F. S., Mitchell C. J., Neu M. Y., Ranshaw L. E., Solanke Y. E., Somers D. O., Wiseman J. O., *Bioorg. Med. Chem. Lett.*, **18**, 4237–4241 (2008).
11) Skoumbourdis A. P., LeClair C. A., Stefan E., Turjanski A. G., Maguire W., Titus S. A., Huang R., Auld D. S., Inglese J., Austin C. P., Michnick S. W., Xia M., Thomas C. J., *Bioorg. Med. Chem. Lett.*, **19**, 3686–3692 (2009).
12) Smith M. T., Crouch N. R., Gericke N., Hirst M., *J. Ethnopharmacol.*, **50**, 119–130 (1996).
13) Harvey A. L., Young L. C., Viljoen A. M., Gericke N. P., *J. Ethnopharmacol.*, **137**, 1124–1129 (2011).
14) Wachtel H., *Neuropharmacology*, **22**, 267–272 (1983).
15) Bobon D., Breulet M., Gerard-Vandenhove M. A., Guiot-Goffioul F., Plomteux G., Sastre-y-Hernandez M., Schratzer M., Troisfontaines B., von Frenckell R., Wachtel H., *Eur. Arch. Psychiatry Neurol. Sci.*, **238**, 2–6 (1988).
16) Griswold D. E., Webb E. F., Breton J., White J. R., Marshall P. J., Torphy T. J., *Inflammation*, **17**, 333–344 (1993).
17) Sommer N., Loschmann P. A., Northoff G. H., Weller M., Steinbrecher A., Steinbach J. P., Lichtenfels R., Meyermann R., Riethmuller A., Fontana A., Dichgans J., Martin R., *Nat. Med.*, **1**, 244–248 (1995).
18) Zhu J., Mix E., Winblad B., *CNS Drug Rev.*, **7**, 387–398 (2001).
19) Boswell-Smith V., Spina D., *Int. J. Chron. Obstruct. Pulmon. Dis.*, **2**, 121–129 (2007).
20) Herbert C., Hettiaratchi A., Webb D. C., Thomas P. S., Foster P. S., Kumar R. K., *Clin. Exp. Allergy*, **38**, 847–856 (2008).
21) Hohlfeld J. M., Schoenfeld K., Lavae-Mokhtari M., Schaumann F., Mueller M., Bredenbroeker D., Krug N., Hermann R., *Pulm. Pharmacol. Ther.*, **21**, 616–623 (2008).
22) Field S. K., *Expert Opin. Investig. Drugs*, **17**, 811–818 (2008).
23) Billah M., Buckley G. M., Cooper N., Dyke H. J., Egan R., Ganguly A., Gowers L., Haughan A. F., Kendall H. J., Lowe C., Minnicozzi M., Montana J. G., Oxford J., Peake J. C., Picken C. L., Piwinski J. J., Naylor R., Sabin V., Shih N. Y., Warneck J. B., *Bioorg. Med. Chem. Lett.*, **12**, 1617–1619 (2002).
24) Billah M., Cooper N., Cuss F., Davenport R. J., Dyke H. J., Egan R., Ganguly A., Gowers L., Hannah D. R., Haughan A. F., Kendall H. J., Lowe C., Minnicozzi M., Montana J. G., Naylor R., Oxford J., Peake J. C., Piwinski J. J., Runcie K. A., Sabin V., Sharpe A., Shih N. Y., Warneck J. B., *Bioorg. Med. Chem. Lett.*, **12**, 1621–1623 (2002).
25) Billah M. M., Cooper N., Minnicozzi M., Warneck J., Wang P., Hey J. A., Kreutner W., Rizzo C. A., Smith S. R., Young S., Chapman R. W., Dyke H., Shih N. Y., Piwinski J. J., Cuss F. M., Montana J., Ganguly A. K., Egan R. W., *J. Pharmacol. Exp. Ther.*, **302**, 127–137 (2002).
26) Woodrow M. D., Ballantine S. P., Barker M. D., Clarke B. J., Dawson J., Dean T. W., Delves C. J., Evans B., Gough S. L., Guntrip S. B., Holman S., Holmes D. S., Kranz M., Lindvaal M. K., Lucas F. S., Neu M., Ranshaw L. E., Solanke Y. E., Somers D. O., Ward P., Wiseman J. O., *Bioorg. Med. Chem. Lett.*, **19**, 5261–5265 (2009).
27) Elansary A. K., Kadry H. H., Ahmed E. M., Sonousi A. S. M., *Med. Chem. Res.*, **21**, 3557–3567 (2012).
28) Castaño T., Wang H., Campillo N. E., Ballester S., González-García C., Hernández J., Pérez C., Cuenca J., Pérez-Castillo A., Martínez A., Huertas O., Gelpí J. L., Luque F. J., Ke H., Gil C., *ChemMedChem*, **4**, 866–876 (2009).
29) Glaser T., Traber J., *Agents Actions*, **15**, 341–348 (1984).
30) Tobe M., Isobe Y., Tomizawa H., Nagasaki T., Obara F., Matsumoto M., Hayashi H., *Chem. Pharm. Bull.*, **50**, 1073–1080 (2002).
31) Ishii N., Shirato M., Wakita H., Miyazaki K., Takase Y., Asano O., Kusano K., Yamamoto E., Inoue C., Hishinuma I., *J. Pharmacol. Exp. Ther.*, **346**, 105–112 (2013).
32) Card G. L., England B. P., Suzuki Y., Fong D., Powell B., Lee B., Luu C., Tabrizizad M., Gillette S., Ibrahim P. N., Artis D. R., Bollag G., Milburn M. V., Kim S. H., Schlessinger J., Zhang K. Y., *Structure*, **12**, 2233–2247 (2004).
33) Jeon Y. H., Heo Y. S., Kim C. M., Hyun Y. L., Lee T. G., Ro S., Cho J. M., *Cell. Mol. Life Sci.*, **62**, 1198–1220 (2005).
34) Rabe K. F., Bateman E. D., O'Donnell D., Witte S., Bredenbroker D., Bethke T. D., *Lancet*, **366**, 563–571 (2005).
35) Calverley P. M., Sanchez-Toril F., McIvor A., Teichmann P., Bredenbroeker D., Fabbri L. M., *Am. J. Respir. Crit. Care Med.*, **176**, 154–161 (2007).
36) Bruno O., Fedele E., Prickaerts J., Parker L. A., Canepa E., Brullo C., Cavallero A., Gardella E., Balbi A., Domenicotti C., Bollen E., Gijselaers H. J., Vanmierlo T., Erb K., Limebeer C. L., Argellati F., Marinari U. M., Pronzato M. A., Ricciarelli R., *Br. J. Pharmacol.*, **164**, 2054–2063 (2011).
37) Woodrow M. D., Ballantine S. P., Barker M. D., Clarke B. J., Dawson J., Dean T. W., Delves C. J., Evans B., Gough S. L., Guntrip S. B., Holman S., Holmes D. S., Kranz M., Lindvaal M. K., Lucas F. S., Neu M., Ranshaw L. E., Solanke Y. E., Somers D. O., Ward P., Wiseman J. O., *Bioorg. Med. Chem. Lett.*, **19**, 5261–5265 (2009).
38) Laddha S. S., Wadodkar S. G., Meghal S. K., *Med. Chem. Res.*, **18**, 268–276 (2009).
39) Endicott M. M., Wick E., Mercury M. L., Sherrill M. L., *J. Am. Chem. Soc.*, **68**, 1299–1301 (1946).
40) Claesen M., Vanderhaeghe H., *Bulletin des Sociétés Chimiques Belges*, **68**, 220–224 (1959).
41) Nomoto Y., Takai H., Ohno T., Kubo K., *Chem. Pharm. Bull.*, **39**, 900–910 (1991).

42) Tworowski D., Matsievitch R., PCT Int. Appl. WO 2007110868 A2, p. 108 (2007).
43) Abou-Seri S. M., Abouzid K., Abou El Ella D. A., *Eur. J. Med. Chem.*, **46**, 647–658 (2011).
44) Srivastav M., Salahuddin M., Shantakumar S. M., *Eur. J. Org. Chem.*, **6**, 1055–1062 (2009).
45) Baker B. R., Patel R. P., *Biochem. Biophys. Res. Commun.*, **9**, 199–203 (1962).
46) George T., Tahilramani R., Mehta D. V., *Indian J. Chem.*, **9**, 1077–1080 (1971).
47) Rees G. S., Gee C. K., Ward H. L., Ball C., Tarrant G. M., Poole S., Bristow A. F., *Eur. Cytokine Netw.*, **10**, 383–392 (1999).
48) Cioli V., Putzolu S., Rossi V., Scorza Barcellona P., Corradino C., *Toxicol. Appl. Pharmacol.*, **50**, 283–289 (1979).
49) Laddha S. S., Bhatnagar S. P., *Bioorg. Med. Chem.*, **17**, 6796–6802 (2009).
50) Esmat A., Al-Abbasi F. A., Algandaby M. M., Moussa A. Y., Labib R. M., Ayoub N. A., Abdel-Naim A. B., *J. Med. Food*, **15**, 278–287 (2012).
51) Holtmann M. H., Schuchmann M., Zeller G., Galle P. R., Neurath M. F., *Arch. Immunol. Ther. Exp.*, **50**, 279–288 (2002).
52) Arai K. I., Lee F., Miyajima A., Miyatake S., Arai N., Yokota T., *Annu. Rev. Biochem.*, **59**, 783–836 (1990).
53) Harada A., Sekido N., Akahoshi T., Wada T., Mukaida N., Matsushima K., *J. Leukoc. Biol.*, **56**, 559–564 (1994).
54) Gamble J. R., Harlan J. M., Klebanoff S. J., Vadas M. A., *Proc. Natl. Acad. Sci. U.S.A.*, **82**, 8667–8671 (1985).
55) Dinarello C. A., *Chest*, **112** (Suppl.), 321S–329S (1997).
56) Thong-Ngam D., Choochuai S., Patumraj S., Chayanupatkul M., Klaikeaw N., *World J. Gastroenterol.*, **18**, 1479–1484 (2012).
57) Deleuze-Masquéfa C., Gerebtzoff G., Subra G., Fabreguettes J. R., Ovens A., Carraz M., Strub M. P., Bompart J., George P., Bonnet P. A., *Bioorg. Med. Chem.*, **12**, 1129–1139 (2004).
58) Xu R. X., Rocque W. J., Lambert M. H., Vanderwall D. E., Luther M. A., Nolte R. T., *J. Mol. Biol.*, **337**, 355–365 (2004).
59) Manallack D. T., Hughes R. A., Thompson P. E., *J. Med. Chem.*, **48**, 3449–3462 (2005).
60) Zhang K. Y., Card G. L., Suzuki Y., Artis D. R., Fong D., Gillette S., Hsieh D., Neiman J., West B. L., Zhang C., Milburn M. V., Kim S. H., Schlessinger J., Bollag G., *Mol. Cell*, **15**, 279–286 (2004).
61) Fox D. 3rd, Burgin A. B., Gurney M. E., *Cell. Signal.*, **26**, 657–663 (2014).
62) Richter W., Unciuleac L., Hermsdorf T., Kronbach T., Dettmer D., *Cell. Signal.*, **13**, 287–297 (2001).
63) Winter C. A., Risley E. A., Nuss G. W., *Proc. Soc. Exp. Biol. Med.*, **111**, 544–547 (1962).
64) Basso N., Materia A., Forlini A., Jaffe B. M., *Surgery*, **94**, 104–108 (1983).
65) Robert A., Nezamis J. E., Phillips J. P., *Gastroenterology*, **55**, 481–487 (1968).
66) Bancroft J. D., Stevens A., "Theory and Practice of Histological Techniques," 2nd ed., Churchil Livingstone, New York, 1982, pp. 438–439.